Universal Curve of Optimum Thermoelectric Figures of Merit for Bulk and Low-Dimensional Semiconductors

Nguyen T. Hung,* Ahmad R. T. Nugraha, and Riichiro Saito
Department of Physics, Tohoku University, Sendai 980-8578, Japan

(Received 26 September 2017; revised manuscript received 19 December 2017; published 20 February 2018)

This paper is a contribution to the Physical Review Applied *collection in memory of Mildred S. Dresselhaus.*

Analytical formulas for thermoelectric figures of merit and power factors are derived based on the one-band model. We find that there is a direct relationship between the *optimum* figures of merit and the optimum power factors of semiconductors despite of the fact that the two quantities are generally given by different values of chemical potentials. By introducing a dimensionless parameter consisting of the optimum power factor and lattice thermal conductivity (without electronic thermal conductivity), it is possible to unify optimum figures of merit of both bulk and low-dimensional semiconductors into a single universal curve that covers many materials with different dimensionalities.

DOI: 10.1103/PhysRevApplied.9.024019

I. INTRODUCTION

Most of the electrical energy that we consume in daily life comes from thermal processes, such as heat engines in cars and power plants, in which more than half of the energy is wasted in the form of heat [1]. Research on thermoelectricity for recovering this waste heat—i.e., converting the waste heat directly into electric energy—is thus of great interest [1,2]. A good thermoelectric (TE) material is characterized by how efficiently the electricity can be obtained for a given heat source, in which the thermoelectric figure of merit $ZT = S^2\sigma\kappa^{-1}T$ is usually evaluated, where S, σ, κ, and T are the Seebeck coefficient, the electrical conductivity, the thermal conductivity, and the average absolute temperature, respectively. It is well known that obtaining the optimum ZT ($ZT_{\rm opt}$ for short) for a certain TE material—where $ZT_{\rm opt}$ is defined as the maximum value of ZT as a function of the chemical potential—is often complicated by the interdependence of S, σ, and κ [3]. Therefore, finding the best material to obtain as large a $ZT_{\rm opt}$ as possible has been a great challenge for many years. As one strategy, using low-dimensional semiconductors with a large density of states at the top of the valence band (or at the bottom of the conduction band) was suggested by Hicks and Dresselhaus to improve $ZT_{\rm opt}$ [4–6]. However, we recently pointed out that, in terms of their power factor $\mathrm{PF} = S^2\sigma$, only low-dimensional semiconductors with confinement lengths smaller than their thermal de Broglie wavelengths prove to be more useful TE materials than the bulk ones [7].

Another strategy to find the best thermoelectric materials is to define a material parameter that can be the most essential one to determine $ZT_{\rm opt}$. We can mention several efforts by researchers who proposed some parameters for evaluating $ZT_{\rm opt}$. For example, in 1996, Mahan and Sofo introduced a dimensionless material parameter k_BT/E_b [8], where k_B and E_b are the Boltzmann constant and the energy bandwidth, respectively. When E_b is infinitesimal, the transport distribution function $\mathcal{T} = v^2\tau\mathcal{D}$ forms a δ function that leads to the largest possible value of $ZT_{\rm opt}$, where v is the carrier velocity, τ is the carrier relaxation time, and $\mathcal{D}$ is the density of states of the carrier at the Fermi energy. This work was revisited from a Landauer perspective by Jeong *et al.* [9], who found that a finite E_b dispersion produces a higher ZT when the lattice thermal conductivity is finite. Much earlier, in 1959, Chasmar and Stratton suggested that a parameter $B = 5.745 \times 10^{-6}(\mu/\kappa_l)(m/m_0)^{3/2}T^{5/2}$, where μ, κ_l, m, and m_0 are the carrier mobility, the lattice thermal conductivity, the carrier effective mass, and the free-electron mass, respectively, determines the optimum ZT [10]. Note that the product of μ and $(m/m_0)^{3/2}$ has commonly been called the weighted mobility. A large B value usually corresponds to a high ZT value at a certain chemical potential. The advantage of the parameter B is that, to obtain a good TE material, instead of checking all of the interdependent transport properties, one should look for a semiconductor with a high weighted mobility and a low lattice thermal conductivity κ_l, which are less dependent on each other. Although E_b and B have been used to guide researches in thermoelectricity for many years, it is not possible to directly identify $ZT_{\rm opt}$ by using only these parameters. On the other hand, there has been a lot of effort dedicated to optimizing the PF, giving the optimum power

*nguyen@flex.phys.tohoku.ac.jp

factor PF_{opt} that can be obtained by changing the chemical potential [11]. Since ZT_{opt} generally occurs at a different chemical potential than the PF_{opt}, i.e., $ZT_{opt} \neq PF_{opt}\kappa^{-1}T$, one always needs to measure or estimate ZT_{opt} independently from the PF_{opt} by rechecking the chemical potential dependence of ZT. Therefore, it should prove to be useful for thermoelectric applications if we can calculate ZT_{opt} from the information of the PF_{opt} or other simple parameters.

In this paper, we propose that an alternative material parameter $\alpha = (PF_{opt}/\kappa_l)T$ can be defined to directly determine ZT_{opt}. Although ZT_{opt} and the PF_{opt} are generally optimized at *different* chemical potentials, the value of ZT_{opt} can be calculated using an analytical formula that involves the so-called Lambert W function, where α can be used as an input parameter. Without loss of generality, the analytical formula for ZT_{opt} is derived within the one-band model and the nondegenerate semiconductor approximation. We show in this paper that ZT_{opt} for both bulk and low-dimensional semiconductors can be unified into a single universal curve, which allows us to predict and understand the materials of different dimensions that can have a better ZT_{opt} value by simply calculating the α parameter.

The rest of this paper is organized as follows. In Sec. II, we start the derivation of some formulas of thermoelectric properties from the conventional Boltzmann transport theory. This initial derivation will give us PF and ZT formulas involving integrals that must be calculated numerically. In Sec. III, we apply a nondegenerate semiconductor approximation so that the PF_{opt} and ZT_{opt} can be obtained analytically, which results in the universal curve of ZT_{opt}. Finally, in Sec. IV, we conclude the paper and give a few perspectives on future work in the field of thermoelectricity. We also provide some appendixes for additional information about the derivation of the formulas and the Lambert W function.

II. THEORETICAL METHODS

By solving the linearized Boltzmann equations within the one-band model and the relaxation-time approximation, three TE transport properties are related to the transport distribution function $\mathcal{T}(E)$ as follows:

$$\sigma = q^2\mathcal{L}_0, \qquad S = \frac{1}{qT}\frac{\mathcal{L}_1}{\mathcal{L}_0}, \qquad \kappa_e = \frac{1}{T}\left(\mathcal{L}_2 - \frac{\mathcal{L}_1^2}{\mathcal{L}_0}\right), \quad (1)$$

where σ, S, and κ_e, are the electrical conductivity, the Seebeck coefficient, and the electronic thermal conductivity, respectively. $\mathcal{L}_i$ is the transport integral that is defined by [8]

$$\mathcal{L}_i = \int \mathcal{T}(E)(E-E_F)^i\left(-\frac{\partial f_0}{\partial E}\right)dE, \text{ with } i = 0,1,2, \quad (2)$$

where E is the energy of carrier and $f_0 = 1/[e^{(E-E_F)/k_BT}+1]$ is the Fermi-Dirac distribution function, where the Fermi energy E_F is defined as the chemical potential measured from the bottom (top) of the conduction (valence) energy band in an n-type (p-type) semiconductor, and $\mathcal{T}(E)$ is defined

$$\mathcal{T}(E) = v_x^2(E)\tau(E)\mathcal{D}(E), \quad (3)$$

where $v_x(E)$, $\tau(E)$, and $\mathcal{D}(E)$ are the group velocity in the x direction, the relaxation time, and the density of states (DOS) of the carrier, respectively.

From Eqs. (1) and (2), the thermoelectric power factor PF and the figure of merit ZT can be written as

$$PF = S^2\sigma = \frac{1}{T^2}\frac{\mathcal{L}_1^2}{\mathcal{L}_0}, \quad (4)$$

$$ZT = \frac{S^2\sigma}{\kappa_e+\kappa_l}T = \beta\frac{\mathcal{L}_1^2}{\mathcal{L}_0\mathcal{L}_2 - \mathcal{L}_1^2}, \quad (5)$$

where κ_l is the lattice thermal conductivity and $\beta = 1/(\kappa_l/\kappa_e + 1) \leq 1$. It is clear from Eqs. (4) and (5) that the PF and ZT have a different dependence on E_F.

For the sake of simplicity, we consider a single parabolic band, in which the energy band structure and the group velocity can be given as $E(\mathbf{k}) = \hbar^2\mathbf{k}^2/2m$ and $v(\mathbf{k}) = (1/\hbar)[\partial E(\mathbf{k})/\partial\mathbf{k}] = \hbar\mathbf{k}/m$, respectively, where $\mathbf{k}$ is the wave vector of the carrier, m is the carrier effective mass, and $\hbar$ is the Planck constant. We assume that the material is isotropic with a certain dimension $d = 1, 2, 3$, the group velocity $v_x^2(E) = v^2(\mathbf{k})/d = \hbar^2\mathbf{k}^2/m^2d = 2E/md$, and the carrier relaxation time is inversely proportional to the carrier DOS [12], $\tau(E) = C\mathcal{D}^{-1}(E)$, where C is the scattering coefficient in units of $W^{-1}\,m^{-3}$. The DOS is defined as $\mathcal{D}(E) = (2/\Omega)\sum_{\mathbf{k}}\delta[E - E(\mathbf{k})]$ in units of $J^{-1}\,m^{-3}$, where the factor 2 accounts for the spin degeneracy and Ω is the volume of the system. Detailed derivations of how we can calculate C for a typical material are given in Appendix A. After substituting $v_x^2(E)$ and $\tau(E)$ into $\mathcal{T}(E)$ in Eq. (3), the integrals $\mathcal{L}_i$ in Eq. (2) can be written as

$$\mathcal{L}_0 = \frac{2C}{md}(k_BT)F_0, \quad (6)$$

$$\mathcal{L}_1 = \frac{2C}{md}(k_BT)^2(2F_1 - \eta F_0), \quad (7)$$

$$\mathcal{L}_2 = \frac{2C}{md}(k_BT)^3(3F_2 - 4\eta F_1 + \eta^2 F_0), \quad (8)$$

where $\eta = E_F/k_BT$ is the reduced (or dimensionless) chemical potential and $F_j(\eta) = \int \eta^j f_0 d\eta$ is the Fermi-Dirac integral. By substituting $\mathcal{L}_i$ from Eqs. (6), (7), and (8)

into Eqs. (4) and (5), we obtain the formulas of the PF and ZT as follows:

$$\mathrm{PF} = \frac{2Ck_B^3T}{md}\frac{(2F_1-\eta F_0)^2}{F_0}, \tag{9}$$

$$ZT = \beta\frac{(2F_1-\eta F_0)^2}{F_0(3F_2-4\eta F_1+\eta^2F_0)-(2F_1-\eta F_0)^2}, \tag{10}$$

where the integrals F_0, F_1, and F_2 are calculated numerically.

III. RESULTS AND DISCUSSION

In this section, we first discuss an example of calculating the PF and ZT as a function of η for one semiconducting material by using Eqs. (9) and (10) numerically. After that, we simplify the PF and ZT formulas by considering nondegenerate semiconductor approximation, which gives us analytical formulas of the $\mathrm{PF_{opt}}$ and ZT_{opt}. The ZT_{opt} formula can then be plotted and compared with various experimental data, leading to a universal curve of ZT_{opt}.

A. Example of a typical material

Figures 1(a)–1(d) show, respectively, the dependence of S and σ, the PF [Eq. (9)], β and κ_l/κ_e, and ZT [Eq. (10)] on the reduced chemical potential η for different dimensions. When plotting Figs. 1(a)–1(d), we consider a typical semiconductor, n-type $Bi_2Te_{2.7}Se_{0.3}$, at $T = 298$ K and a doping concentration of about 0.92×10^{19} cm^{-3}. The carrier effective mass, the carrier mobility, and the lattice thermal conductivity are taken to be $m = 1.12m_0$, $\mu = 173$ cm^2/V s, and $\kappa_l = 0.728$ W/mK, respectively, for the 3D ($d = 3$) bulk n-type $Bi_2Te_{2.7}Se_{0.3}$ [13]. The scattering coefficient $C = 1.18\times10^{33}$ W^{-1}m^{-3} is obtained from m and μ by using Eq. (A13) from Appendix A, which leads to an average relaxation time of about 0.1 ps. We temporarily use the same parameter values of m, κ_l, and C for the 1D ($d = 1$) and 2D ($d = 2$) systems as for the 3D ones. However, these parameters generally vary by dimension for different materials, which we adopt in Sec. III C.

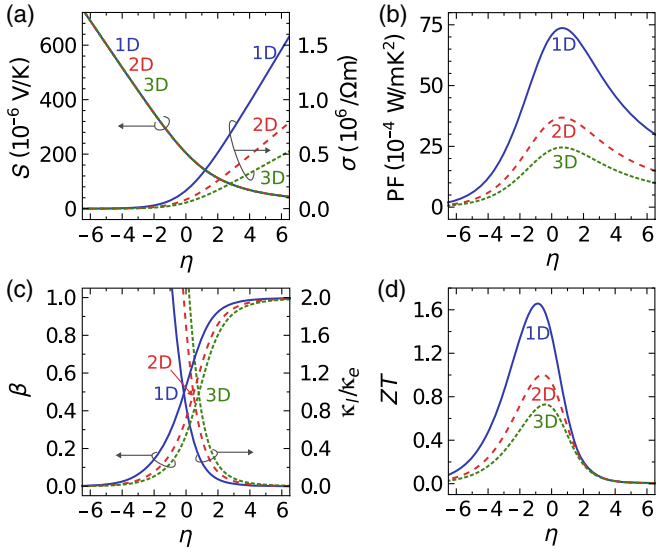

FIG. 1. (a) S and σ, (b) the PF, (c) β and κ_l/κ_e, and (d) ZT as a function of the reduced chemical potential η for the 1D, 2D, and 3D systems, respectively. The carrier effective mass, the carrier mobility, and the lattice thermal conductivity are set at $m = 1.12m_0$, $\mu = 173$ cm^2/V s, and $\kappa_l = 0.728$ W/mK, respectively, for n-type $Bi_2Te_{2.7}Se_{0.3}$ at room temperature ($T = 298$ K) [13].

Figure 1(a) shows that S is independent of d and increases with a decreasing η value, while σ depends on d and decreases with a decreasing η value. This behavior can be understood in terms of their units since the units (V/K) of S show no dependence of length scale, while the units (1/Ωm) of σ show a dependence of length scale. Figure 1(b) shows a strong enhancement of the maximum PF around $\eta \approx 0$ in the low-dimensional systems (1D and 2D). For the bulk (3D) system, the theoretical maximum PF value is about 0.0025 W/mK^2, which is in a good agreement with the experimental data of about 0.0021 W/mK^2 [13]. In the case of $\eta \gg 0$, we can see that S approaches zero because the system becomes metallic at high doping concentrations, while σ is close to zero when $\eta \ll 0$ [Fig. 1(a)]. Therefore, the $\mathrm{PF_{opt}}$ occurs at $\eta \approx 0$, in which E_F lies at the bottom (top) of the conduction (valence) energy band in a p-type (n-type) semiconductor for all of the 1D, 2D, and 3D systems, as shown in Fig. 1(b). Figure 1(d) shows a strong enhancement of the maximum ZT values in the 1D and 2D systems, which is known as the Hicks-Dresselhaus theory [4,5]. For the 3D system, the theoretical maximum ZT value is about 0.72, which is in a good agreement with the experimental data of about 0.73 [13]. In the case of $\eta \gg 0$, the coefficient $\beta = 1/(\kappa_l/\kappa_e + 1) \approx 1$ since k_e is much larger than k_l when the system is metallic, as shown in Fig. 1(c). By contrast, $\beta \approx 0$ when $\eta \ll 0$ because k_e is near zero (few free-electron carriers in the insulators) [see Fig. 1(c)]. Therefore, ZT_{opt} is found at $\eta < 0$, in which E_F lies in the energy gap, as shown in Fig. 1(d). Important information for Figs. 1(b) and 1(d) is that the PF and ZT are optimized at $\eta \approx 0$ and $\eta < 0$, respectively, for all 1D, 2D, and 3D systems, although the two quantities are located at *different* η values for each d value.

B. Nondegenerate semiconductor approximation

Next, we would like to obtain the analytical formulas for both the $\mathrm{PF_{opt}}$ and ZT_{opt}. In Eqs. (9) and (10), which are used to plot Figs. 1(b) and 1(d), we consider the full solutions of Fermi-Dirac integrals F_0, F_1, and F_2 numerically. The problem is, how can we get analytical formulas for the $\mathrm{PF_{opt}}$ and ZT_{opt} to approach these two quantities?

Since the PF_{opt} (ZT_{opt}) is optimized at $\eta \approx 0$ ($\eta < 0$), we may use the nondegenerate semiconductor approximation that is especially valid for $\eta \leq 0$ [14]. In this case, the Fermi-Dirac integral is approximated as $F_j(\eta) \approx e^{\eta}\Gamma(j+1)$ [14], where $\Gamma(j)$ is the Γ function. By substituting $F_0 = e^{\eta}$, $F_1 = e^{\eta}$, and $F_2 = 2e^{\eta}$ into Eq. (9), we get the PF formula

$$\mathrm{PF} = \frac{2Ck_B^3T}{md}(2-\eta)^2 e^{\eta}. \tag{11}$$

Since $\kappa_e = (1/T)(\mathcal{L}_2 - \mathcal{L}_1^2/\mathcal{L}_0) = 4Ck_B^3T^2e^{\eta}/(md)$ [see Eq. (1)], β can be written as

$$\beta = \frac{1}{[2/(\alpha e^{\eta})] + 1}, \tag{12}$$

where

$$\alpha = \frac{8Ck_B^3T^2}{md\kappa_l} \tag{13}$$

is a dimensionless parameter. Substituting β into Eq. (10) and applying the approximation of F_j, we obtain

$$ZT = \frac{(2-\eta)^2}{[4/(\alpha e^{\eta})] + 2}. \tag{14}$$

In Figs. 2(a) and 2(b), respectively, we show the PF_{opt} and ZT_{opt} that are calculated based on the full solutions of Fermi-Dirac integrals [Eqs. (9) and (10)] and the nondegenerate semiconductor approximation [Eqs. (11) and (14)]. If we focus solely on the *values* of the PF_{opt} and ZT_{opt} (local maxima of the PF and ZT) at $\eta \leq 0$, we can see that the analytical formulas based on the nondegenerate semiconductor approximation can nicely reproduce the PF_{opt} and ZT_{opt} of the full solutions. Therefore, we can

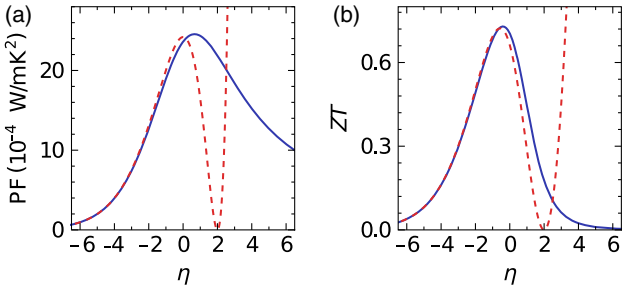

FIG. 2. (a) The PF and (b) ZT as functions of the reduced chemical potential η. Results from the formulas involving numerical integrations and those from an analytical calculation (a nondegenerate semiconductor approximation) are represented by solid and dashed lines, respectively. The carrier effective mass, the carrier mobility, and the lattice thermal conductivity are set at $m = 1.12m_0$, $\mu = 173$ cm^2/V s, and $\kappa_l = 0.728$ W/mK, respectively, for 3D n-type $Bi_2Te_{2.7}Se_{0.3}$ at room temperature [13].

determine the PF_{opt} and ZT_{opt} from Eqs. (11) and (14) by solving $d(\mathrm{PF})/d\eta = 0$ and $d(ZT)/d\eta = 0$, respectively. The formulas obtained for the PF_{opt} and ZT_{opt} are

$$\mathrm{PF}_{opt} = \frac{8Ck_B^3T}{md}, \qquad ZT_{opt} = \frac{W_0^2(\alpha)}{2} + W_0(\alpha), \tag{15}$$

where $W_0(\alpha)$ is the principal branch of the Lambert W function (see Appendix B). By substituting the PF_{opt} from Eq. (15) into Eq. (13), the α parameter is now expressed in terms of the PF_{opt} and κ_l,

$$\alpha = \frac{\mathrm{PF}_{opt}}{\kappa_l}T. \tag{16}$$

The corresponding reduced chemical potentials for the PF_{opt} and ZT_{opt} are $\eta_{opt}^{PF} = 0$ and $\eta_{opt}^{ZT} = -W_0(\alpha)$, respectively (see Fig. 2). Based on the simple analytical formulas in Eq. (15), the values of the PF_{opt} and ZT_{opt} can be calculated directly from C, d, m, κ_l, and T, which could be measured in experiments. For example, in the case of 3D n-type $Bi_2Te_{2.7}Se_{0.3}$ at room temperature, taken from Ref. [13], we have $C = 1.18 \times 10^{33}$ W^{-1} m^{-3} (see also Appendix A), $d = 3$, $m = 1.12m_0$, and $\kappa_l = 0.728$ W/mK, and hence $PF_{opt} = 0.0024$ W/mK^2 and $ZT_{opt} = 0.72$. This analytical result agrees well with both the fully numerical calculation ($PF_{opt} = 0.0025$ W/mK^2 and $ZT_{opt} = 0.72$) (see Fig. 2) and the experimental data ($PF_{opt} = 0.0021$ W/mK^2 and $ZT_{opt} = 0.73$) [13].

To gain insight into the PF_{opt}, we can substitute the coefficient C from Eq. (A13) in Appendix A into the PF_{opt} formula in Eq. (15), so that the PF_{opt} is given by

$$\mathrm{PF}_{opt} = \frac{16\mu k_B^2}{qL^3}\left(\frac{L}{\Lambda}\right)^d \frac{\Gamma(\frac{5}{2})}{\Gamma(\frac{7-d}{2})\Gamma(\frac{d}{2})}, \tag{17}$$

where L is the confinement length for a particular material dimension, and $\Lambda = [2\pi\hbar^2/(mk_BT)]^{1/2}$ is the thermal de Broglie wavelength (a measure of the thermodynamic uncertainty for the localization of an electron or hole of mass m) [15]. Equation (17) shows the dependence of the PF_{opt} on μ, d, L, and Λ. By scaling the PF_{opt} with the optimum PF of a 3D system, i.e., PF_{opt}^{3D}, we find that the ratio PF_{opt}/PF_{opt}^{3D} merely depends on the factor $(L/\Lambda)^{d-3}$, which is consistent with our previous work [7]. It is clear that the PF_{opt} is enhanced for 1D and 2D semiconductors only when L is smaller than Λ. Interestingly, in this work, we find that by defining $\alpha = (PF_{opt}/\kappa_l)T$, we can have a direct relation of ZT_{opt} with the PF_{opt} through Eq. (15). Note that $W_0(\alpha)$ monotonically increases with α, as shown in Fig. 4. It is important to point out that the factor $(L/\Lambda)^{d-3}$ is the enhancement factor not only of the PF_{opt} but also of ZT_{opt} for the low-dimensional semiconductors.

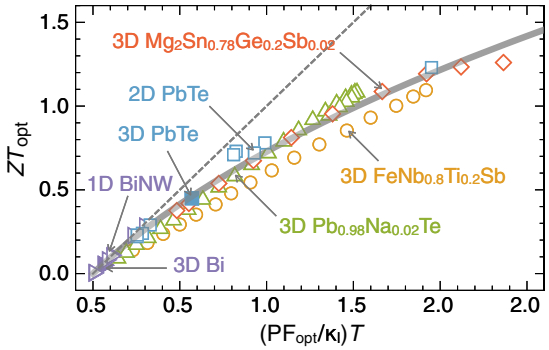

FIG. 3. ZT_{opt} as a function of $\alpha = (PF_{opt}/\kappa_l)T$. The solid line denotes the theoretical curve from Eq. (15), while the dashed line is the plot of $ZT_{opt} = \alpha$ and serves as a guide for the eye. The symbols represent experimental results of 1D Bi nanowires (right-pointing open triangle) and 3D Bi (right-pointing filled triangle) [16], 2D PbTe quantum wells (open square) and 3D PbTe (filled square) [17], 3D $Pb_{0.98}Na_{0.02}Te$ (up-pointing triangle) [18], 3D $FeNb_{0.8}Ti_{0.2}Sb$ (open circle) [19], and 3D $Mg_2Sn_{0.78}Ge_{0.2}Sb_{0.02}$ (diamond) [20].

C. The universal curve

Let us now compare the ZT_{opt} formula with various experimental data. In Fig. 3, we plot theoretical ZT_{opt} (the solid curve) as a function of α [Eq. (15)]. Here, ZT_{opt} merely depends on the PF_{opt}, κ_l, and T, despite the fact that the PF and ZT are optimized at different chemical potentials, i.e., $\eta_{opt}^{PF} = 0$ and $\eta_{opt}^{ZT} = -W_0(\alpha)$, respectively. Hence, ZT_{opt} from various materials with different dimensions can be compared directly with the theoretical curve. The experimental data (the symbols) in Fig. 3 are extracted from plots of ZT_{opt}, the PF_{opt}, and κ_l in Refs. [16–20] by using digitizer software. These data include 1D Bi nanowires of different diameters (approximately 38–290 nm) along with bulk 3D Bi at room temperature [16], 2D PbTe quantum wells of different thicknesses (roughly 1.9–4.0 nm) along with 3D PbTe at room temperature [17], and also 3D $Pb_{0.98}Na_{0.02}Te$ [18], 3D $FeNb_{0.8}Ti_{0.2}Sb$ [19], and 3D $Mg_2Sn_{0.78}Ge_{0.2}Sb_{0.02}$ [20] at different temperatures (about 300–1100 K).

As can be seen in Fig. 3, all experimental data tend to fit the theoretical curve from Eq. (15). The values of ZT_{opt} monotonically increase as a function of α, and thus we can say that any semiconductor should have the material parameter $\alpha > 4.5$ to obtain $ZT_{opt} > 2$. At smaller α values (a higher T value or a higher PF_{opt}), we have $\eta_{opt}^{ZT} \sim \eta_{opt}^{PF}$, especially at around $\alpha < 0.3$. In this case, $ZT_{opt} \sim (PF_{opt}/\kappa_l)T$ (see the dotted line in Fig. 3). On the other hand, at larger α values, we have $\eta_{opt}^{ZT} < \eta_{opt}^{PF}$, which eventually results in a nonlinear function of ZT_{opt} versus $(PF_{opt}/\kappa_l)T$. The main benefit of using the universal curve in Fig. 3 is that it provides an alternative way to directly calculate ZT_{opt} from the PF_{opt} and κ_l without needing to check the electron thermal conductivity κ_e or the optimum chemical potential η_{opt}^{ZT}.

IV. CONCLUSION

We show in this paper that the simple analytical formulas [Eq. (15)] based on the one-band model can directly relate the optimum figures of merit ZT_{opt} with the optimum power factors PF_{opt} of semiconductors. By introducing the material parameter $\alpha = (PF_{opt}/\kappa_l)T$, we can obtain the universal curve of ZT_{opt} combining both bulk and low-dimensional semiconductors, in which ZT_{opt} monotonically increases as a function of α. Since this approach reduces parameters such as κ_e and η_{opt}^{ZT} in the calculation of ZT_{opt}, we believe that it will help researchers to better identify alternative thermoelectric materials in the future.

ACKNOWLEDGMENTS

N. T. H. and A. R. T. N thank Dr. E. H. Hasdeo for the fruitful discussions and acknowledge the financial support from the Interdepartmental Doctoral Degree Program for Multi-dimensional Materials Science Leaders, Tohoku University. R. S. acknowledges JSPS KAKENHI Grants No. JP25107005 and No. JP25286005. R. S. also thanks the late Prof. M. S. Dresselhaus for long-lasting collaborations and for introducing thermoelectricity to the authors.

APPENDIX A: THE SCATTERING COEFFICIENT C

1. Defining C from Fermi's "golden rule"

Fermi's golden rule gives the scattering rate of transitions between discrete states $|\mathbf{k}\rangle$ and $|\mathbf{k}'\rangle$ as follows [21]:

$$\frac{1}{\tau(\mathbf{k} \to \mathbf{k}')} \approx \frac{2\pi}{\hbar} |\langle \mathbf{k}'|V|\mathbf{k}\rangle|^2 \delta[E(\mathbf{k}) - E(\mathbf{k}')], \quad \text{(A1)}$$

where $\hbar$ is the Planck constant, V is the perturbation potential, δ is the Dirac-δ function, and E is the energy dispersion. The general scattering rate is given by the product $2\pi/\hbar$ times the square of the transition matrix element times a Dirac-δ function. For the one-band model, the scattering rate is between states within the parabolic energy band, where a *continuum* of states exist. In this case, the final scattering rate is obtained by a summation over all relevant states,

$$\frac{1}{\tau(\mathbf{k})} = \sum_{\mathbf{k}'} \frac{1}{\tau(\mathbf{k} \to \mathbf{k}')} = \frac{2\pi}{\hbar} \sum_{\mathbf{k}'} |\langle \mathbf{k}'|V|\mathbf{k}\rangle|^2 \delta[E(\mathbf{k}) - E(\mathbf{k}')]. \quad \text{(A2)}$$

As an example, consider the scattering rate between electron states in the conduction band due to a point scatterer in a 3D semiconductor. Let us consider a perturbing potential $V(\mathbf{r}) = V_0 \delta(\mathbf{r})$ for short-range interactions, where V_0 is constant in units of $J\,m^3$. The

matrix element between electronic states $|\mathbf{k}\rangle$ and $|\mathbf{k}'\rangle$ can be obtained as [22]

$$|\langle\mathbf{k}'|V_0\delta(\mathbf{r})|\mathbf{k}\rangle| = \int d^3\mathbf{r}\left(\frac{e^{-i\mathbf{k}'\cdot\mathbf{r}}}{\sqrt{\Omega}}\right)V_0\delta(\mathbf{r})\left(\frac{e^{+i\mathbf{k}'\cdot\mathbf{r}}}{\sqrt{\Omega}}\right) = \frac{V_0}{\Omega}, \tag{A3}$$

where Ω is the volume of the system. After substituting the matrix element from Eq. (A3) into Eq. (A2), the scattering rate can be written as

$$\frac{1}{\tau(\mathbf{k})} = \frac{2\pi}{\hbar}\left(\frac{V_0}{\Omega}\right)^2\sum_{\mathbf{k}'}\delta[E(\mathbf{k}) - E(\mathbf{k}')]. \tag{A4}$$

By using the carrier DOS, defined as $\mathcal{D}(E) = (2/\Omega)\sum_{\mathbf{k}}\delta[E - E(\mathbf{k})]$ in units of $\mathrm{J}^{-1}\,\mathrm{m}^{-3}$, where the factor 2 accounts for the spin degeneracy, Eq. (A4) is now expressed as

$$\frac{1}{\tau(E)} = \frac{\pi V_0^2}{\hbar\Omega}\mathcal{D}(E). \tag{A5}$$

This example shows an important result indicating that the scattering rate for the continuum of states is, in general, proportional to the DOS, while the strength of scattering increases with the square of the scattering potential. The carrier relaxation time $\tau(E)$ is thus inversely proportional to the carrier DOS:

$$\tau(E) = C\mathcal{D}^{-1}(E), \tag{A6}$$

where $C = \hbar\Omega/(\pi V_0^2)$ is the scattering coefficient in units of $\mathrm{W}^{-1}\,\mathrm{m}^{-3}$. Note that, according to Fermi's golden rule, the coefficient C can be a constant value when the matrix element is approximately constant.

2. Calculating C from experimental data

Here, we derive a formula of the coefficient C considering a parabolic band for any semiconductor so that C can be calculated from the experimental data. The carrier relaxation time $\tau(E)$ and the density of states $\mathcal{D}(E)$ per unit volume are, respectively, defined by [14,22]

$$\tau(E) = \tau_0\left(\frac{E}{k_BT}\right)^r, \tag{A7}$$

$$\mathcal{D}(E) = \frac{(2m/\hbar^2)^{d/2}E^{d/2-1}}{L^{3-d}2^{d-1}\pi^{d/2}\Gamma(\frac{d}{2})}, \tag{A8}$$

where k_B is the Boltzmann constant, T is the average absolute temperature, τ_0 is the carrier relaxation-time coefficient, r is a characteristic exponent, $d = 1, 2, 3$ denotes the dimension of the system, m is the carrier effective mass, and L is the confinement length for a particular material dimension. For a given $\tau(E)$ value, the carrier mobility is defined by

$$\mu = \frac{q\langle\langle\tau(E)\rangle\rangle}{m}. \tag{A9}$$

The average relaxation time is defined by [22]

$$\langle\langle\tau(E)\rangle\rangle \equiv \frac{\langle E\tau(E)\rangle}{\langle E\rangle} = \tau_0\frac{\Gamma(\frac{5}{2}+r)}{\Gamma(\frac{5}{2})}, \tag{A10}$$

where Γ is the Γ function. From Eqs. (A7), (A9), and (A10), the carrier relaxation time $\tau(E)$ can be rewritten as

$$\tau(E) = \frac{\mu m\Gamma(\frac{5}{2})}{q\Gamma(\frac{5}{2}+r)}\left(\frac{E}{k_BT}\right)^r. \tag{A11}$$

We assume that the acoustic phonon scattering is the main carrier scattering mechanism at room temperature, i.e., $\tau(E) \propto \mathcal{D}(E)^{-1}$ [12,22]. From Eqs. (A8) and (A11) and $\tau(E) \propto \mathcal{D}(E)^{-1}$, we obtain $r = 1 - d/2$ for the system with dimension d. By using $r = 1 - d/2$ from Eqs. (A6), (A8), and (A11), the coefficient C can be written as

$$\begin{aligned} C &= \tau(E)\mathcal{D}(E) \\ &= \frac{2\mu m\Gamma(\frac{5}{2})}{qk_BTL^{3-d}\Gamma(\frac{7-d}{2})\Gamma(\frac{d}{2})}\left(\frac{mk_BT}{2\pi\hbar^2}\right)^{d/2}. \end{aligned} \tag{A12}$$

After substituting the thermal de Broglie wavelength $\Lambda = (2\pi\hbar^2/mk_BT)^{1/2}$ into Eq. (A12), the coefficient C is given by

$$C = \frac{2\mu m}{qk_BTL^3}\left(\frac{L}{\Lambda}\right)^d\frac{\Gamma(\frac{5}{2})}{\Gamma(\frac{7-d}{2})\Gamma(\frac{d}{2})}. \tag{A13}$$

Equation (A13) is useful for calculating the coefficient C from μ and m, which can be obtained from the experimental data. For example, in the 3D ($d = 3$) n-type $Bi_2Te_{2.7}Se_{0.3}$ [13], at room temperature ($T = 298$ K) and a doping concentration on the order of 10^{19} cm^3, the carrier mobility and the carrier effective mass are $\mu = 173$ $\mathrm{cm}^2/\mathrm{V\,s}$ and $m = 1.12m_0$, respectively, where m_0 is the free-electron mass. From Eq. (A13), we obtain a C value of about 1.18×10^{33} $\mathrm{W}^{-1}\,\mathrm{m}^{-3}$ and, correspondingly, the average relaxation time is about 0.1 ps.

APPENDIX B: THE LAMBERT W FUNCTION

The Lambert W function is defined as a multivalued complex function that satisfies the following equation:

$$W(\alpha) = \alpha e^{-W(\alpha)}, \quad \text{where } \alpha \in \mathbb{C}. \tag{B1}$$

Equation (B1) always has an infinite number of solutions in the complex plane—hence the multivaluedness of the W

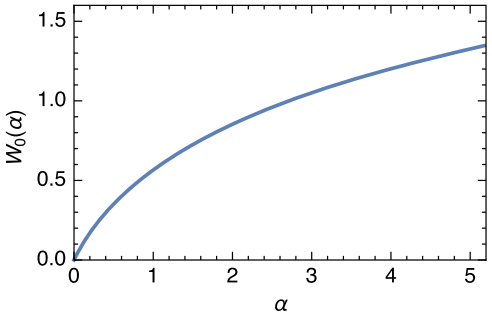

FIG. 4. The real principal branch of the W function in the case of $a \in [0, \infty)$.

function. These solutions are indexed by the integer variable j and are called the branches of the W function, W_j, for $j \in \mathbb{Z}$. Specifically, the solutions of Eq. (B1) in the calculation of ZT_{opt} correspond to $\alpha \in [0, \infty)$. In this case, there can be a real solution corresponding to the principal branch of the W function, i.e., $W_0(\alpha) \in [0, \infty)$.

The W_0 function can be written in terms of the series expansion as follows [23]:

$$W_0(\alpha) = \sum_{n=1}^{\infty} \frac{(-n)^{n-1}}{n!}\alpha^n = \alpha - \alpha^2 + \frac{3}{2}\alpha^3 - \frac{8}{3}\alpha^4 + \frac{125}{24}\alpha^5 - \frac{54}{5}\alpha^6 + \frac{16\,807}{720}\alpha^7 + \cdots. \quad \text{(B2)}$$

Figure 4 shows $W_0(\alpha)$ as a function of α when $\alpha \in [0, \infty)$.

[1] L. E. Bell, Cooling, heating, generating power, and recovering waste heat with thermoelectric systems, Science **321**, 1457 (2008).

[2] J. P. Heremans, M. S. Dresselhaus, L. E. Bell, and D. T. Morelli, When thermoelectrics reached the nanoscale, Nat. Nanotechnol. **8**, 471 (2013).

[3] C. B. Vining, An inconvenient truth about thermoelectrics, Nat. Mater. **8**, 83 (2009).

[4] L. D. Hicks and M. S. Dresselhaus, Effect of quantum-well structures on the thermoelectric figure of merit, Phys. Rev. B **47**, 12727 (1993).

[5] L. D. Hicks and M. S. Dresselhaus, Thermoelectric figure of merit of a one-dimensional conductor, Phys. Rev. B **47**, 16631 (1993).

[6] L. D. Hicks, T. C. Harman, X. Sun, and M. S. Dresselhaus, Experimental study of the effect of quantum-well structures on the thermoelectric figure of merit, Phys. Rev. B **53**, R10493 (1996).

[7] N. T. Hung, E. H. Hasdeo, A. R. T. Nugraha, M. S. Dresselhaus, and R. Saito, Quantum Effects in the Thermoelectric Power Factor of Low-Dimensional Semiconductors, Phys. Rev. Lett. **117**, 036602 (2016).

[8] G. D. Mahan and J. O. Sofo, The best thermoelectric, Proc. Natl. Acad. Sci. U.S.A. **93**, 7436 (1996) [http://www.pnas.org/content/93/15/7436].

[9] C. Jeong, R. Kim, and M. S. Lundstrom, On the best bandstructure for thermoelectric performance: A Landauer perspective, J. Appl. Phys. **111**, 113707 (2012).

[10] R. P. Chasmar and R. Stratton, The thermoelectric figure of merit and its relation to thermoelectric generators, J. Electron. Control **7**, 52 (1959).

[11] H. J. Goldsmid, *Introduction to Thermoelectricity* (Springer-Verlag, Berlin, 2010).

[12] J. Zhou, R. Yang, G. Chen, and M. S. Dresselhaus, Optimal Bandwidth for High Efficiency Thermoelectrics, Phys. Rev. Lett. **107**, 226601 (2011).

[13] W. S. Liu, Q. Zhang, Y. Lan, S. Chen, X. Yan, Q. Zhang, H. Wang, D. Wang, G. Chen, and Z. Ren, Thermoelectric property studies on Cu-doped n-type $Cu_xBi_2Te_{2.7}Se_{0.3}$ nanocomposites, Adv. Energy Mater. **1**, 577 (2011).

[14] N. T. Hung, A. R. T. Nugraha, E. H. Hasdeo, M. S. Dresselhaus, and R. Saito, Diameter dependence of thermoelectric power of semiconducting carbon nanotubes, Phys. Rev. B **92**, 165426 (2015).

[15] C. Kittel and H. Kroemer, *Thermal Physics* (W. H. Freeman, San Francisco, 1980).

[16] J. Kim, S. Lee, Y. M. Brovman, P. Kim, and W. Lee, Diameter-dependent thermoelectric figure of merit in single-crystalline Bi nanowires, Nanoscale **7**, 5053 (2015).

[17] T. C. Harman, D. L. Spears, and M. J. Manfra, High thermoelectric figures of merit in PbTe quantum wells, J. Electron. Mater. **25**, 1121 (1996).

[18] L. D. Zhao, H. J. Wu, S. Q. Hao, C. I. Wu, X. Y. Zhou, K. Biswas, J. Q. He, T. P. Hogan, C. Uher, C. Wolverton, V. P. Dravid, and M. G. Kanatzidis, All-scale hierarchical thermoelectrics: MgTe in PbTe facilitates valence band convergence and suppresses bipolar thermal transport for high performance, Energy Environ. Sci. **6**, 3346 (2013).

[19] C. Fu, T. Zhu, Y. Liu, H. Xie, and X. Zhao, Band engineering of high performance p-type FeNbSb based half-Heusler thermoelectric materials for figure of merit $ZT > 1$, Energy Environ. Sci. **8**, 216 (2015).

[20] W. Liu, J. Zhou, Q. Jie, Y. Li, H. S. Kim, J. Bao, G. Chen, and Z. Ren, New insight into the material parameter B to understand the enhanced thermoelectric performance of $Mg_2Sn_{1-x-y}Ge_xSb_y$, Energy Environ. Sci. **9**, 530 (2016).

[21] J. M. Ziman, *Principles of the Theory of Solids* (Cambridge University Press, New York, 1972).

[22] M. Lundstrom, *Fundamentals of Carrier Transport* (Cambridge University Press, New York, 2009).

[23] C. Carathéodory, *Theory of Functions of a Complex Variable* (AMS Chelsea Publishing, New York, 1954).